








## Low-lying resonances in $^{26}\text{Si}$ relevant for the determination of the astrophysical $^{25}\text{Al}(p, \gamma)^{26}\text{Si}$ reaction rate

J. F. Perello <sup>\*</sup>, S. Almaraz-Calderon <sup>†</sup>, B. W. Asher, L. T. Baby, C. Benetti, K. W. Kemper , E. Lopez-Saavedra, G. W. McCann , A. B. Morelock, V. Tripathi , and I. Wiedenhöver 

*Department of Physics, Florida State University, Tallahassee, Florida 32306, USA*

B. Sudarsan 

*Department of Physics and Astronomy, Louisiana State University, Baton Rouge, Louisiana 70803, USA*

 (Received 26 September 2021; revised 13 January 2022; accepted 22 February 2022; published 24 March 2022)

The  $^{25}\text{Al}(p, \gamma)^{26}\text{Si}$  reaction plays a key role in accurately modeling and understanding the nucleosynthesis of the long-lived radioisotope  $^{26}\text{Al}$  observed throughout the galaxy by  $\gamma$ -ray telescopes via the detection of its 1.809 MeV  $\gamma$ -ray line. The  $^{25}\text{Al}(p, \gamma)^{26}\text{Si}$  reaction is responsible for redirecting the flux of nuclear material away from the ground state of the long-lived radioisotope  $^{26}\text{Al}$  ( $^{26}\text{Al}^g$ ) in favor of its short-lived isomer ( $^{26}\text{Al}^m$ ) which bypasses the emission of the 1.809 MeV  $\gamma$  ray, but is observed in, for example, an excess of the isotopic abundance of  $^{26}\text{Mg}$  in meteorites. Uncertainties in the  $^{25}\text{Al}(p, \gamma)^{26}\text{Si}$  reaction rate are dominated by the nuclear properties of low-lying proton-unbound states in  $^{26}\text{Si}$ . A high-sensitivity spectroscopic study of  $^{26}\text{Si}$  was performed at the John D. Fox Accelerator Laboratory at Florida State University, using a neutron/ $\gamma$ -ray coincidence measurement with the  $^{24}\text{Mg}(^3\text{He}, n\gamma)^{26}\text{Si}$  reaction. The present measurement solves previous discrepancies in the existence and location of the relevant resonances in  $^{26}\text{Si}$ . Furthermore, the high sensitivity of the study allowed for a direct estimate of the  $3_3^+$   $\gamma$ -partial width. The present experimental information combined with previous works provide an updated rate of the  $^{25}\text{Al}(p, \gamma)^{26}\text{Si}$  reaction at nova temperatures.

DOI: [10.1103/PhysRevC.105.035805](https://doi.org/10.1103/PhysRevC.105.035805)

### I. INTRODUCTION

The satellite-based observation of the long-lived radioisotope  $^{26}\text{Al}$  ( $t_{1/2} = 7.17 \times 10^5$  yr), the first of its kind made in space via the detection of characteristic  $\gamma$ -ray lines, has long been recognized as direct evidence that stellar nucleosynthesis processes are ongoing in the galaxy [1]. The observation of  $^{26}\text{Al}$  via the 1.809 keV  $\gamma$ -ray line also explains the excess of  $^{26}\text{Mg}$  found in presolar dust grains on meteorites [2,3]. The spatial distribution of  $^{26}\text{Al}$   $\gamma$ -ray intensity mapped by the COMPTEL [4] and INTEGRAL [5] space missions estimate an equilibrium mass of  $\approx 2$ – $3$  solar masses of  $^{26}\text{Al}$  currently present in the Milky Way, with  $^{26}\text{Al}$  been accumulated in regions of star formation and corotating with the plane of the galaxy.

The understanding of the nucleosynthesis of galactic  $^{26}\text{Al}$  is elemental in various research areas and has the potential of being used as, for example, a high-resolution chronometer of events during the time of planetary formation in the galaxy [6]; a method to estimate the rate of core collapse supernovae (CCSN) explosions [7]; to identify the stellar origin of

presolar grains with high inferred  $^{26}\text{Al}/^{27}\text{Al}$  ratios [3]; or to benchmark models of massive star nucleosynthesis [1,8].

The suggested sites for production of  $^{26}\text{Al}$  are predominantly massive Wolf-Rayet (WR) stars and their subsequent CCSN phase [1,8]. However, the observed  $^{60}\text{Fe}/^{26}\text{Al}$  ratio of their  $\gamma$ -ray fluxes is significantly smaller than theoretical predictions when compared to CCSN models, supporting the hypothesis that there are other important sources of  $^{26}\text{Al}$  in the galaxy [3,9].

Classical nova explosions, one of the most frequent types of thermonuclear explosions in the galaxy ( $\approx 40$  per year [10]), are expected to contribute up to 30% to the nucleosynthesis of  $^{26}\text{Al}$  [11]. In classical novae,  $^{26}\text{Al}$  is produced via the  $^{24}\text{Mg}(p, \gamma)^{25}\text{Al}(\beta^+)^{25}\text{Mg}(p, \gamma)^{26}\text{Al}$  reaction chain [12]. However, a key uncertainty in novae nucleosynthesis models for understanding  $^{26}\text{Al}$  is the  $^{25}\text{Al}(p, \gamma)^{26}\text{Si}$  reaction, which competes with the  $\beta$  decay of  $^{25}\text{Al}$  at peak nova burning temperatures [13].

The  $^{25}\text{Al}(p, \gamma)^{26}\text{Si}$  reaction and the subsequent  $\beta$  decay of  $^{26}\text{Si}$  leads predominantly to the population of  $^{26}\text{Al}$  in its short-lived isomeric state ( $^{26}\text{Al}^m$ ,  $t_{1/2} = 6.4$  s) rather than its ground state ( $^{26}\text{Al}^g$ ,  $t_{1/2} = 7.17 \times 10^5$  yr).  $^{26}\text{Al}^m$  ( $0^+$ )  $\beta$  decays directly to the ground state of  $^{26}\text{Mg}$  ( $0^+$ ), bypassing the 1.809 MeV  $\gamma$ -ray emission. Therefore, it is possible for  $^{26}\text{Al}$  to contribute to the  $^{26}\text{Mg}$  abundance measured in pre-solar grains and meteorites without space telescopes observing its associated  $\gamma$  ray. Hence, a reliable calculation of the rate of the  $^{25}\text{Al}(p, \gamma)^{26}\text{Si}$  proton-capture reaction is

<sup>\*</sup>Present address: Intelligence and Space Research Division, Los Alamos National Laboratory, Los Alamos, NM 87545, USA; [jperello@lanl.gov](mailto:jperello@lanl.gov)

<sup>†</sup>[salmarazcalderon@fsu.edu](mailto:salmarazcalderon@fsu.edu)

TABLE I. Properties of the first five proton resonance states in  $^{26}\text{Si}$ . Adapted from Ref. [18].

| Resonance | $E_{ex}$ (keV)   | $J^\pi$          | $E_r$ (keV)     |
|-----------|------------------|------------------|-----------------|
| 1         | $5517.3 \pm 0.8$ | $4_4^+$          | $3.5 \pm 0.9$   |
| 2         | $5675.2 \pm 1.4$ | $1_1^+$          | $161.4 \pm 1.5$ |
| 3         | $5890.0 \pm 0.8$ | $(0_4^+)$        | $376.2 \pm 1.0$ |
| 4         | $5927.6 \pm 1.0$ | $3_3^+$          | $413.8 \pm 1.1$ |
| 5         | $5949.7 \pm 5.3$ | $(4_5^+, 0_4^+)$ | $435.9 \pm 5.3$ |

critical to the understanding of the net production of  $^{26}\text{Al}$  in the galaxy [14].

Direct measurements of astrophysical reactions at stellar energies are very challenging, if at all possible, due to the very small cross sections of the reactions of interest and the radioactive nature of nuclei involved [15]. Indirect methods are commonly used to calculate the rate of the reactions in explosive stellar environments as is the case for the  $^{25}\text{Al}(p, \gamma)^{26}\text{Si}$  reaction, which is dominated at nova temperatures ( $T \approx 0.1\text{--}0.4$  GK) by low-lying resonance states in  $^{26}\text{Si}$  ( $S_p = 5514$  keV [16]). Considerable experimental and theoretical efforts have been aimed to identify the relevant resonances and their nuclear properties [13,14,17–35]. However, these efforts have not been without controversy. In the most recent compilation by Chipps [18], five low-lying proton resonances in  $^{26}\text{Si}$  were highlighted that could play a role in the calculation of the  $^{25}\text{Al}(p, \gamma)^{26}\text{Si}$  reaction rate at nova temperatures. The properties of these resonances are summarized in Table I. These values are taken as averages over all the reported findings.

The  $4_4^+$  state has been confirmed at  $5517.3(8)$  keV [20]. However, the contribution of this state to the astrophysical reaction rate is negligible due to its location just a few keV above the proton threshold in  $^{26}\text{Si}$ , placing it well below the Gamow window for novae temperatures. Most recent experiments [13,19,21–25] are in good agreement regarding the location and spin-parity of the  $1^+$ ,  $0^+$ , and  $3^+$  states, placing them at  $E_{ex} = 5675.2(14)$  keV,  $E_{ex} = 5890.0(8)$  keV, and  $E_{ex} = 5927.6(10)$  keV, respectively.

Significant experimental efforts have gone into measuring the partial width of the  $3^+$  state [13,19,21,23,26] giving that it has the largest resonant strength, which makes the reaction rate strongly dependent on it. The  $\gamma$  partial width for this state has only been recently observed in two independent  $\beta$ -decay studies of  $^{26}\text{P}$  [19,23] by detecting the  $3_3^+ \rightarrow 3_2^+$   $\gamma$ -ray transition ( $E_\gamma = 1741$  keV) in coincidence with the  $\beta$  decay. The resonant strength extracted from these studies are  $23 \pm 6(\text{stat})$  meV and  $34.5 \pm_{15.7}^{17.0}(\text{stat})$  meV, respectively. However, this transition has not been observed in other reaction studies due to the state’s extremely small ( $\approx 2\%$ ) ratio of  $\gamma$ -partial width to the total width of the state ( $\Gamma_\gamma/\Gamma$ ).

Additionally, conflicting evidence of a possible resonance near  $E_{ex} = 5950$  keV and its spin-parity assignment still remains. A state at this energy was first observed by Caggiano *et al.* [35] in 2002 (assigning a  $3^+$ ) and was later identified in 2004 by Parpottas *et al.* [26] as a  $0^+$  using the  $^{24}\text{Mg}(^3\text{He}, n)$  reaction. Theoretical studies do not predict two closely spaced  $0^+$  states in this region [28,30]. It has been

suggested by Ref. [18] that possible “intruder” states could be present, which to date has not been considered in theoretical calculations. From mirror assignments, one expects another  $4^+$  to be near this region, but the analysis of the data from Ref. [26] ruled out a  $J = 4$  assignment. A  $2^+$  resonance is not expected in this region [18,30], eliminating the possibility of an even-parity assignment for this state. Most recently, a study performed on the stable  $^{26}\text{Mg}$  mirror system by Canete *et al.* [27] suggested that this state could be the lowest  $1^-$  state, adding to the discrepancies and uncertainties on the nuclear properties of resonances in  $^{26}\text{Si}$ .

The experimental discrepancies in this energy region even among studies using the same reaction mechanism performed at similar energies, point out to a misinterpretation of the observed states. The ( $^3\text{He}, n$ ) reaction study in 2004 by Parpottas *et al.* [26], identified the  $0^+$  at  $E_{ex} = 5946(4)$  keV, and the  $3^+$  at  $E_{ex} = 5916(4)$  keV. Recent ( $^3\text{He}, n\gamma$ ) reactions studies [22,24,25], which ran at the same energy as Ref. [26], placed the  $0^+$  at  $E_{ex} = 5890.0(8)$  keV, contradicting the placement by Ref. [26]. Moreover, Parpottas *et al.* did not report a state at  $E_{ex} = 5890$  keV which has been observed in subsequent similar studies. A possible explanation could be a shift in energy calibration by Ref. [26] of around  $\approx 26$  keV in this energy region. This shift would reconcile the energies of the states reported by Ref. [26] with the ones reported by other ( $^3\text{He}, n$ ) reactions [22,24,25]. It should be pointed out that a flip in the spin assignments by Ref. [26] would also be needed for full agreement of the different data sets. Additional evidence for the energy and spin assignments of states in  $^{26}\text{Si}$  comes from a ( $p, t$ ) experiment performed in 2010 [34]. This experiment also observed a state at  $5921(12)$  and  $5944(20)$  keV, but was unable to assign a  $J^\pi$ . The existence and spin-parity of a state near  $E_{ex} = 5950$  keV in  $^{26}\text{Si}$  is still an open question.

This work reports on a measurement of the  $^{24}\text{Mg}(^3\text{He}, n\gamma)^{26}\text{Si}$  reaction using a highly sensitive neutron/ $\gamma$ -ray coincidence measurement to populate low-lying resonance states in  $^{26}\text{Si}$  at the same reaction energy as Refs. [24–26]. The nonselective nature of the ( $^3\text{He}, n$ ) reaction allowed population of all relevant resonances in  $^{26}\text{Si}$ . A set of high-purity germanium detectors measured  $\gamma$  rays from de-excitations of populated states in  $^{26}\text{Si}$ . The neutrons from the reaction were measured in a state-of-the-art deuterated liquid scintillator array, which provided pulse-height capabilities additional to the traditional pulse-shape-discrimination and time-of-flight methods resulting in an increased sensitivity from previous similar studies. These results allow the resolution of outstanding discrepancies in the calculation of the  $^{25}\text{Al}(p, \gamma)^{26}\text{Si}$  reaction rate in novae environments.

## II. EXPERIMENT

The experiment was performed at the John D. Fox Accelerator Laboratory at Florida State University (FSU). A 10 MeV stable  $^3\text{He}$  beam from the FN Tandem accelerator was used to bombard an enriched,  $492 \mu\text{g}/\text{cm}^2$  self-supported  $^{24}\text{Mg}$  target, which was placed inside a thin, cylindrical, aluminum reaction chamber. The beam was bunched with a period of 82.5 ns, with a width of 1.7 ns. Typical intensi-

ties of the  $^3\text{He}$  beam on target of  $\approx 15$  nA were observed during the duration of the experiment. The unreacted  $^3\text{He}$  beam was dumped 2 m downstream from the target onto a beam stop consisting of a thick graphite block. The beam stop was surrounded with borated polyethylene, water, and lead sheets to reduce beam induced background. Neutrons from the  $^{24}\text{Mg}(^3\text{He}, n\gamma)^{26}\text{Si}$  reaction were measured with neutron detectors from the compound array for transfer reactions in nuclear astrophysics (CATRiNA). The CATRiNA array consists of 16  $\text{C}_6\text{D}_6$  deuterated liquid scintillators of the type EJ315 [36]. The scintillating material in the CATRiNA detectors is encapsulated in a 4 in.-diameter  $\times$  2 in.-deep aluminum cylinder coupled to a photomultiplier tube. Additional to the pulse-shape discrimination (PSD) and time-of-flight (ToF) information capabilities of traditional liquid scintillators, the CATRiNA detectors provide pulse-height (PH) information due to the anisotropic nature of the  $d + n$  scattering, which can be related to the energy of the incoming neutrons. Details on the CATRiNA detectors can be found in Ref. [37].

CATRiNA was placed at a distance of 1 m from the target, covering an angular range of  $\pm 40^\circ$  (solid angle of  $\approx 130$  msr) and centered at  $0^\circ$ . The beam-pipe ran through the center of CATRiNA towards the beam stop, so the neutron detector closest to the beam axis was located at  $14^\circ$ .  $\gamma$  rays from the de-excitations of populated states in  $^{26}\text{Si}$  were measured with a set of three FSU high-purity germanium (HPGe)  $\gamma$ -ray detectors (FSU Clovers), which were placed at  $90^\circ$  from the target and provided high-resolution  $\gamma$ -ray detection. For the present measurement, the signals from the CATRiNA and FSU Clover detectors were coupled using registered events in CAEN V1725/V1730 digitizers [38,39]. Four boards were dedicated to the detectors and were operated in self-triggering mode, where events were built offline using the timestamps of the signals. The clocks of all digitizers were synchronized to the internal clock of the first board (master).

The energy and efficiency calibrations of the Clover detectors were performed using a calibrated  $^{152}\text{Eu}$  source. For the energy calibration, a linear function was fit to several well known  $\gamma$  rays (2.7 keV resolution at 1408 keV) and was later verified using higher energy  $\gamma$  rays from room background and induced activities with negligible deviations (less than 1 keV) at 4.2 MeV. For the efficiency calibrations, the eight strongest  $\gamma$  rays from the  $^{152}\text{Eu}$  source were used [40], yielding a relative efficiency log curve.

The accelerator's 6.0625 MHz radio frequency (rf) signal, used to obtain the neutron time-of-flight (ToF) information, was registered in a V1730 [39] board that was externally triggered by the OR of all CATRiNA signals. An offline event builder, optimized for the present experiment, was used to correlate the events, and build neutron and  $\gamma$ -ray coincidences. Only single crystal  $\gamma$ -ray events were used since the BGO signals from the FSU Clover detectors were VETOed in the offline analysis. Further details about the experimental setup, electronic logic, and event building can be found in Ref. [41].

### III. ANALYSIS AND RESULTS

Neutron events were separated from  $\gamma$ -ray interactions in the neutron detectors using the PSD capabilities of the

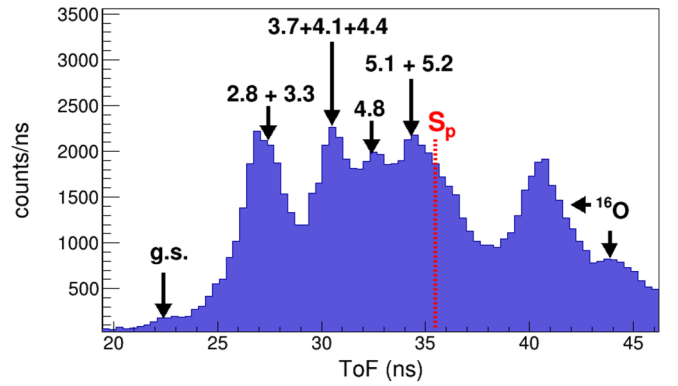


FIG. 1. Neutron-gated ToF spectrum obtained in the present experiment with the CATRiNA detector placed at  $40^\circ$ . Neutron groups corresponding to states in  $^{26}\text{Si}$  as well as groups from  $^{16}\text{O}$  present in the target are labeled (states in  $^{26}\text{Si}$  are given in units of MeV). The dashed vertical line indicates the proton separation energy in  $^{26}\text{Si}$ .

CATRiNA detectors. A PSD threshold was individually set for each neutron detector, which was placed around 350 keVee. ToF information was obtained using the rf signal of the accelerator as reference, including events within a ToF window of two beam bunches (165 ns). The prompt  $\gamma$ -ray peak was used to calibrate the ToF spectrum. A portion of a neutron-gated, calibrated ToF spectrum for one of the neutron detectors is shown in Fig. 1, where the prompt  $\gamma$ -ray peak was placed at 3.3 ns (not visible in the figure). Several neutron energy groups corresponding to excited states in  $^{26}\text{Si}$  are identified in Fig. 1. Peaks from the main contaminant reaction,  $^{16}\text{O}(^3\text{He}, n)$ , are also identified at higher ToF.

Using the  $Q$  value of the reaction ( $Q_{\text{g.s.}} = 70$  keV), a kinematic correction was applied to each neutron detector such that a total  $Q$ -value spectrum from all detectors is obtained. A reconstructed  $Q$ -value spectrum from all 16 neutron detectors is shown in Fig. 2. The  $Q$ -value axis closely approximates the negative of the excitation energy in  $^{26}\text{Si}$  ( $E_{\text{ex}} = -Q + 70$  keV). The proton-separation energy in  $^{26}\text{Si}$  ( $S_p = 5514$  keV) is shown by the dashed vertical red line. States to the left of the  $S_p$  line correspond to resonances in  $^{26}\text{Si}$ .

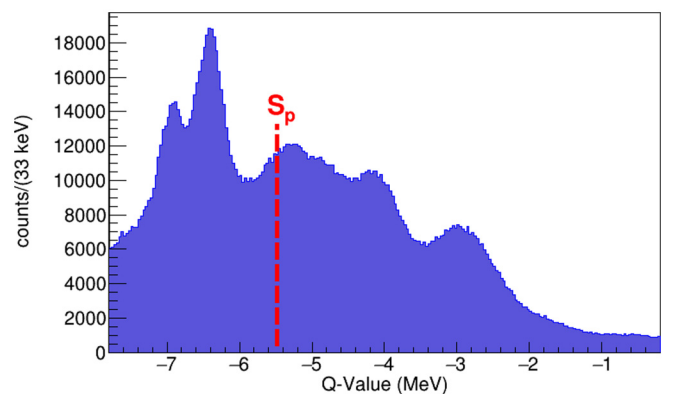


FIG. 2. Reconstructed  $Q$ -value spectrum of the  $^{24}\text{Mg}(^3\text{He}, n\gamma)^{26}\text{Si}$  reaction for all CATRiNA detectors. The dashed vertical line indicates the proton separation energy in  $^{26}\text{Si}$ .

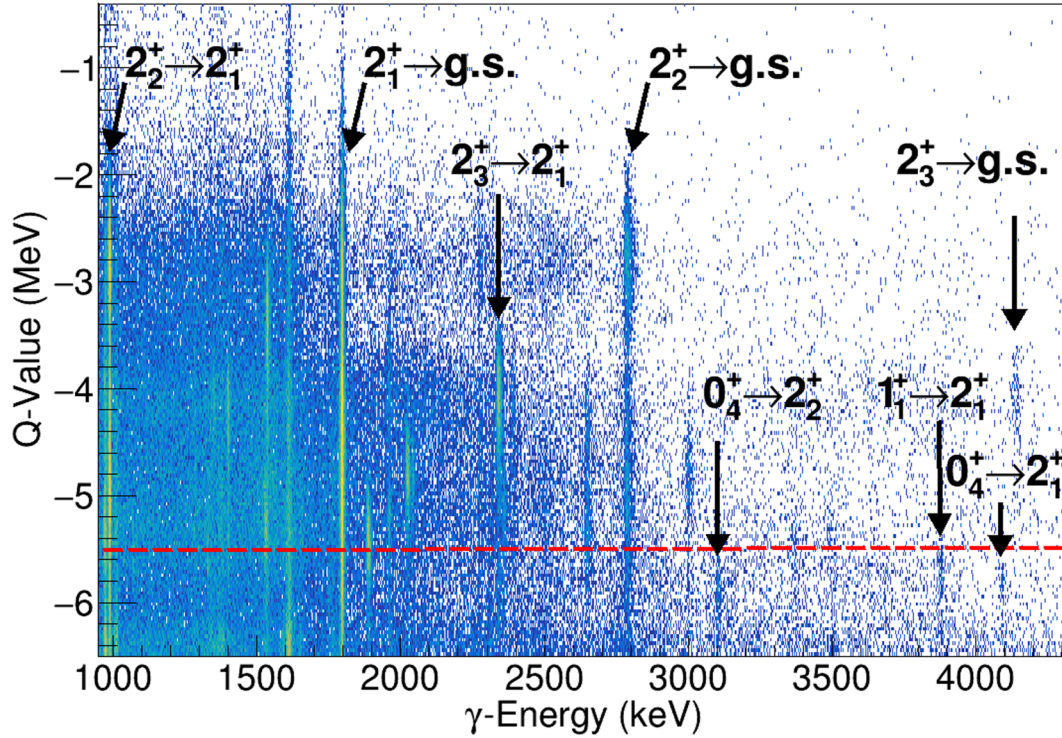


FIG. 3. The neutron- $\gamma$  matrix built using data from the CATRiNA detectors (neutron  $Q$  value in the  $y$  axis) and the FSU Clovers ( $\gamma$ -ray energy in the  $x$  axis). Several well-known transitions in  $^{26}\text{Si}$  are identified. The horizontal red dashed line indicates the proton separation energy ( $S_p$ ) in  $^{26}\text{Si}$ .

A two-dimensional  $n$ - $\gamma$  matrix containing information of  $\gamma$ -ray events in coincidence with neutron events was built with the  $Q$  value of the neutrons in the  $y$  axis and the energy of the  $\gamma$  rays in coincidence with these neutrons in the  $x$  axis. A portion of this  $n$ - $\gamma$  matrix is shown in Fig. 3, where several well-known transitions in  $^{26}\text{Si}$  are identified. Resonance states in  $^{26}\text{Si}$ , the emphasis of this work, are located above the proton-separation energy, which is below the negative  $Q$ -value region indicated by the red-dotted line in Fig. 3.

In this region, we observed two clear transitions from the  $0_4^+$  state ( $0_4^+ \rightarrow 2_2^+$ ,  $E_\gamma = 3103$  keV and  $0_4^+ \rightarrow 2_1^+$ ,  $E_\gamma = 4092$  keV) and one from the  $1_1^+$  state ( $1_1^+ \rightarrow 2_1^+$ ,  $E_\gamma = 3879$  keV). It is important to notice that these two states in  $^{26}\text{Si}$  can only be separated given the high resolution of the  $\gamma$ -ray detectors since the neutron detectors alone would not be able to distinguish between them.

By gating on the highest energy transition from the  $0_4^+$  state ( $E_\gamma = 4092$  keV) and projecting the data to the  $Q$ -value axis (as shown in Fig. 4) we obtain the energy of this state in  $^{26}\text{Si}$  to be  $E_{ex} = 5.90 \pm 0.15$  MeV ( $E_x = Q_{g.s.} - Q_{0^+} = 0.07$  MeV +  $5.83$  MeV =  $5.9$  MeV), which is in agreement with the previously identified state by Doherty *et al.* [25] using  $\gamma$ - $\gamma$  coincidence analysis. Similarly, gating on the  $3879$  keV  $\gamma$ -ray associated to the  $1_1^+$ , we find a  $Q$  value of  $-5.62$  MeV, placing this state at  $E_{ex} = 5.69 \pm 0.18$  MeV, in good agreement with the most recent ( $^3\text{He}$ ,  $n\gamma$ ) experiments [22,24,25]. A  $\gamma$ -ray spectrum gated on neutrons with  $Q$  values corresponding to resonance states in  $^{26}\text{Si}$  (states below the red line in Fig. 3), is shown in Fig. 5. The transitions from the  $4_4^+$

( $E_\gamma = 1072$  keV,  $1330$  keV,  $2733$  keV),  $0_4^+$  ( $E_\gamma = 1751$  keV,  $3103$  keV,  $4092$  keV), and  $1_1^+$  ( $E_\gamma = 2890$  keV,  $3878$  keV) resonance states are clearly visible. The excitation levels from  $\gamma$  rays and neutrons (not available for the  $4^+$  and  $3^+$ ), along with observed  $\gamma$ -decay energies of low-lying resonances are summarized in Table II.

A recent experiment by Canete *et al.* [27] performed on the mirror  $^{26}\text{Mg}$  suggested the existence of a  $1_1^-$  resonance that would correspond to a state at  $E_{ex} = 5.95$  MeV in  $^{26}\text{Si}$ , predicted with a  $\Gamma_\gamma/\Gamma$  of  $\approx 32\%$ , which decays through the  $1_1^- \rightarrow 0_2^+$  transition in  $^{26}\text{Si}$  (100% branching ratio) and emits a  $\gamma$  ray of  $E_\gamma = 2614$  keV [42]. In the present experiment, we

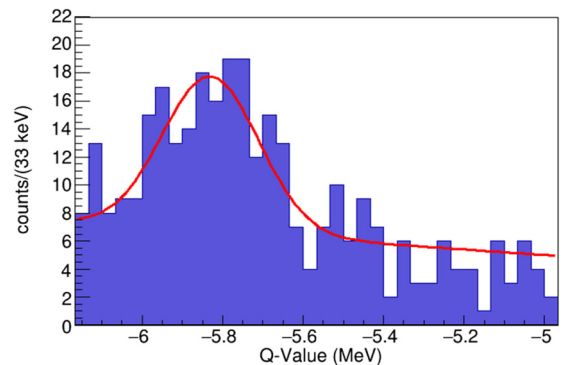


FIG. 4. Neutrons in coincidence with  $\gamma$  rays at  $E_\gamma = 4092$  keV showing a state at  $Q = -5.83$  (15) MeV, which corresponds to  $E_{ex} = 5.90$  MeV in  $^{26}\text{Si}$ .

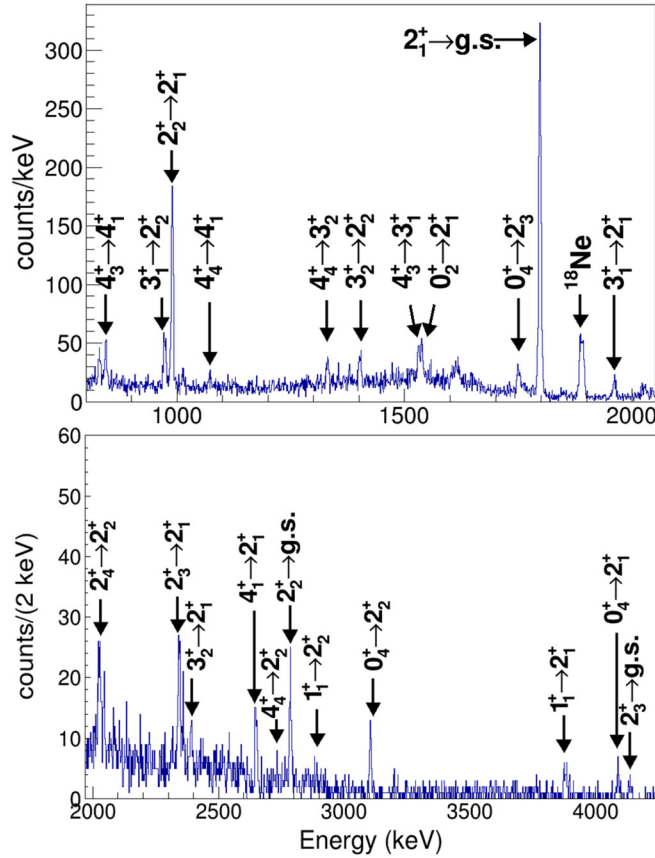


FIG. 5.  $\gamma$  rays in coincidence with neutrons from resonance states in  $^{26}\text{S}$  (states below red line in Fig. 3) with energies below 2 MeV (top) and above 2 MeV (bottom).

did not find evidence of a  $\gamma$ -ray transition with such energy and intensity as shown in Fig. 5.

One of the longstanding questions in the structure of  $^{26}\text{Si}$  is the existence, and  $\gamma$ -partial width of the  $3_3^+$  state. The  $3_3^+$  is expected to undergo a  $3_3^+ \rightarrow 3_2^+$  transition with the emission of a 1741 keV  $\gamma$  ray  $\approx 70\%$  of the  $\gamma$  width based on data from the mirror level in  $^{26}\text{Mg}$  [17,28]. Evidence of a peak at  $E_\gamma = 1741$  keV is observed when constraining the  $Q$  value

TABLE II. Excitation energy levels from  $\gamma$  rays and neutrons (where available), along with  $\gamma$ -decay energy of low-lying resonances.

| $E_{ex}^\gamma$ (keV) | $E_{ex}^n$ (keV) | $E_\gamma$ (keV)                         | $J^\pi$ |
|-----------------------|------------------|--|---------|
| 5517(2)               |                  | 1072(2)<br>1330(2)<br>1763(2)<br>2733(3) | $4_4^+$ |
| 5676(3)               | 5690(180)        | 2890(4)<br>3878(3)                       | $1_1^+$ |
| 5889(2)               | 5900(150)        | 1751(2)<br>3103(2)<br>4092(3)            | $0_4^+$ |
| 5929(3)               |                  | 1741(3)                                  | $3_3^+$ |

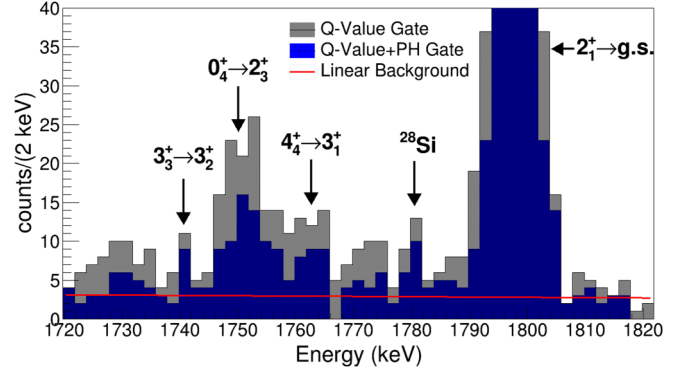


FIG. 6. Portion of the  $\gamma$ -ray spectrum around  $E_\gamma = 1741$  keV corresponding to the  $3_3^+$  resonance state in  $^{26}\text{Si}$ . A neutron gate with neutrons that populated states near  $E_x = 5.9$  MeV,  $Q$  value =  $-5.85 \pm 0.15$  MeV is applied (gray). An additional gate on the PH values centered on  $\text{PH} = 800 \pm 250$  keVee, corresponding to  $E_n = 3.4$ – $3.6$  MeV, was applied (blue). A linear background fit to the blue data is shown by the solid red line.

in the neutron detectors to a region around  $-5.85$  MeV. A portion of the  $\gamma$ -ray spectrum gated with neutrons with  $Q$  values in the range of  $-6.0$  MeV to  $-5.70$  MeV is shown in Fig. 6 (gray). Near the region of 1741 keV, two known transitions from resonance states in  $^{26}\text{Si}$  are observed, the  $E_\gamma = 1751$  keV from the  $0_4^+ \rightarrow 2_3^+$  decay and the  $E_\gamma = 1763$  keV from the  $4_4^+ \rightarrow 3_1^+$  decay. To further determine if the structure at  $E_\gamma = 1741$  keV is associated with the  $E_{ex} = 5.92$  MeV state, the unique PH properties of the CATRINA detectors were used to place an additional gate on the data. Neutrons from the  $3_3^+$  state have energies of  $E_n = 3.4$ – $3.6$  MeV, depending on the angle of the detector. From a neutron ToF-PH correlation matrix, the corresponding PH values for these neutrons were found to be around of  $\approx 800 \pm 250$  keVee, as shown in Fig. 7 for a neutron detector at  $40^\circ$ . The result of the additional neutron PH gate applied to the data is shown in blue in Fig. 6. One can observe that, while the overall statistics

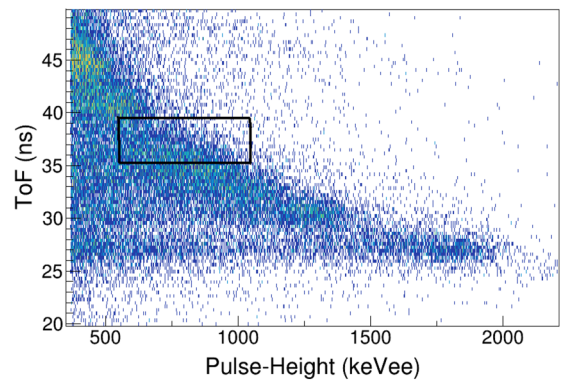


FIG. 7. ToF vs PH correlation matrix obtained in the measurement of the  $^{24}\text{Mg}(^3\text{He}, n\gamma)^{26}\text{Si}$  reaction for the CATRINA detector placed at  $40^\circ$ . An additional gate on the PH values centered on  $\text{PH} = 800 \pm 250$  keVee (shown in black), was applied to all the neutron detectors. This gate corresponds to neutron energies of  $E_n = 3.4$ – $3.6$  MeV, that populate states around  $E_{ex} \approx 5.9$  MeV in  $^{26}\text{Si}$ .

in the spectrum are reduced by a factor of  $\approx \times 0.5$ , the peak at  $E_\gamma = 1741$  keV remains at 86% of its original value (seven counts above background to six counts above background after PH gate), providing additional evidence that it corresponds to the  $3_3^+ \rightarrow 3_2^+$  transition of the state at  $E_{ex} = 5.92$  MeV in  $^{26}\text{Si}$ . For comparison, when applying the PH gate the neighbor structure at 1729 keV is reduced to 20% (166 to 24 counts above background) of its original value, while the  $0^+$ , the  $4^+$ , and the  $2^+$  remain at 56%, 48%, and 56% their original value, respectively.

#### IV. LOW-LYING RESONANCES IN $^{26}\text{Si}$

In the present experiment, low-lying proton resonances in  $^{26}\text{Si}$  relevant in the calculation of the  $^{25}\text{Al}(p, \gamma)^{26}\text{Si}$  reaction rate at nova temperatures were populated via the  $^{24}\text{Mg}(^3\text{He}, n\gamma)^{26}\text{Si}$  reaction. In the following, we summarized the findings of the present experiment for each of the five resonances discussed in Table I.

- (i)  $4_4^+$ . All reported  $\gamma$ -ray transitions for the  $4_4^+$  state were observed in this work. We place the energy level of the  $4_4^+$  resonance in  $^{26}\text{Si}$  at  $E_{ex} = 5517(2)$  keV by analyzing the transition energies. This result is in agreement with recent  $\gamma$ -ray experiments [20,24,25].
- (ii)  $1_1^+$ . Using the neutron  $Q$  value and the  $\gamma$ -ray energy, we report the  $1_1^+$  state at  $E_{ex} = 5676(3)$  keV in  $^{26}\text{Si}$ . This result is in good agreement with most recent ( $^3\text{He}, n\gamma$ ) experiments [22,24,25].
- (iii)  $0_4^+$ . One of the open questions identified by Chipps [18] was the location of the  $0_4^+$  state in  $^{26}\text{Si}$ . Parpottas *et al.* [26] placed their  $0_4^+$  state at  $E_{ex} = 5946(4)$  keV using a ( $^3\text{He}, n$ ) reaction at the same reaction energy as the one used in the present measurement. In this work, the  $0_4^+$  state was observed in the neutron detectors centered at  $Q$  value =  $-5.83(0.15)$  MeV ( $E_{ex} = 5.9$  MeV). By using the added sensitivity of the  $\gamma$ -ray detectors, we report the  $0_4^+$  state at  $E_{ex} = 5889(2)$  keV in  $^{26}\text{Si}$ , in good agreement with recent ( $^3\text{He}, n$ ) experiments [22,24,25] and in disagreement with the work by Parpottas *et al.* [26].
- (iv)  $3_3^+$ . We observe evidence of the peak at 1741(3) keV which agrees well with the reported value by Refs. [19,23] for the  $3_3^+ \rightarrow 3_2^+$  transition, placing the state at  $E_x = 5929(3)$  keV in  $^{26}\text{Si}$ . The 1741 keV transition had only been observed in  $\beta$ -decay experiments. This peak was observed at neutron  $Q$  value and in agreement with the previously reported values by Refs. [13,21,32].
- (v) State at  $E_{ex} = 5950$  keV. In the present work, we do not observe evidence of a state at  $E_{ex} = 5950$  keV in  $^{26}\text{Si}$ , in disagreement with Refs. [26,27]. The  $0_4^+$  state reported by Parpottas *et al.* [26] was placed at  $E_{ex} = 5889(2)$  keV in this work, while the  $\gamma$  transitions suggested by Canete *et al.* [27] from a  $1^-$  state were not found.

In order to extract the  $\gamma$ -partial width ( $\Gamma_\gamma$ ) of the  $3_3^+$  resonant state, we compared the intensities in the  $E_\gamma = 1741$  keV

and  $E_\gamma = 1751$  keV peaks assuming the same  $\gamma$ -ray and neutron detection efficiencies for both states. The 1751 keV  $\gamma$  ray corresponds to the  $0_4^+ \rightarrow 2_3^+$  transition with a measured  $\gamma$  branching of 16% of the total  $0_4^+$   $\gamma$  decay [33]. The  $0_4^+$  resonance has an estimated  $\Gamma_\gamma/\Gamma$  of 64%, calculated using the  $\Gamma_\gamma$  obtained in this work (see Sec. V) and the  $\Gamma_p$  reported by [31]. The  $3_3^+ \rightarrow 3_2^+$  transition is estimated to depopulate the  $3_3^+$  state 71% of the time based on the  $\gamma$  decay of the mirror level in  $^{26}\text{Mg}$  [17]. Since the intensities of the  $0^+$  and the  $3^+$  depend on the reaction mechanism used to populate them and are obtained in this work from a ( $^3\text{He}, n\gamma$ ) coincidence measurement, they will be labeled as  $n\gamma$  intensities. Depending on the relative cross section for both the  $3_3^+$  and the  $0_4^+$  states, the relative intensity between both states can vary. Using the information observed in Parpottas *et al.* [26] work, the  $0_4^+$  state (lowest energy peak) is populated 2–5 times as much as the  $3_3^+$  state (highest energy peak), assuming that the cross sections do not vary much between 8 MeV and 10 MeV incident energy (the peaks are not resolved at 10 MeV). This is the only experiment to provide ( $^3\text{He}, n$ ) cross sections for both states.

The ratio of the counts ( $\frac{3_3^+}{0_4^+}$ ) in the 1741 keV and 1751 keV peaks was found to be  $(6.7 \pm 1.3) \times 10^{-2}$ . Using  $\gamma$ -branching values of 16% and 71% for the  $0^+$  and the  $3^+$ , respectively, a relative  $n\gamma$  intensity of  $1.50 \pm 0.28\%$  is calculated. An absolute  $n\gamma$  intensity of  $3.8 \pm 1.7\%$  was estimated assuming that the  $3_3^+$  is populated about 25–50 % as much as the  $0_4^+$ , as shown in the work by Parpottas *et al.* [26], where the uncertainty in the relative cross sections is incorporated in the error. Combining this information with the 64%  $\Gamma_\gamma/\Gamma$  of the  $0_4^+$ , we report a  $\Gamma_\gamma/\Gamma$  of  $2.5 \pm 1.1\%$  for the  $3_3^+$  state. The use of the relative cross sections from Ref. [26] is the largest uncertainty in this calculation. To reduce this, the cross sections at 10 MeV and at the angles of interest are needed to accurately extract a ratio between both states.

Previous  $\Gamma_\gamma$  values for the  $3_3^+$  state obtained from  $\beta$ -decay experiments by Bennett *et al.* [23] and Liang *et al.* [19], are  $40 \pm 11$  meV and  $60.4 \pm_{27.6}^{30.0}$  meV, respectively. These values used a  $\Gamma_p = 2.9 \pm 1.0$  eV reported by Ref. [13] in 2009. Using the same  $\Gamma_p$ , we report a  $\Gamma_\gamma = 71 \pm 32$  meV, which agrees within error bars, with the two independent  $\beta$ -decay experiments. This value is in rough agreement within one standard deviation with the reported  $\gamma$ -partial width by Canete *et al.* [27] of  $33 \pm 5$  meV, which was calculated using the lifetime of the mirror state in  $^{26}\text{Mg}$ . This discrepancy may be due to the large uncertainty of the relative cross sections between the  $0^+$  and  $3^+$  resonance states used to calculate  $\Gamma_\gamma/\Gamma$  in this work, as well as the  $\approx 35\%$  uncertainty of the  $\Gamma_p$  from Ref. [13] used to extract  $\Gamma_\gamma$ .

#### V. THE $^{25}\text{Al}(p, \gamma)^{26}\text{Si}$ REACTION RATE

The results from the present experiment are used to calculate the rate of the  $^{25}\text{Al}(p, \gamma)^{26}\text{Si}$  proton-capture reaction. From the five resonances listed in Table I, resonance 1  $4_4^+$  at  $E_{ex} = 5517$  KeV is well below the Gamow window at nova temperatures, making its contribution negligible. In the present experiment, we do not observe evidence for resonance 5 at  $E_{ex} = 5.945$  MeV and it will not be included in the present

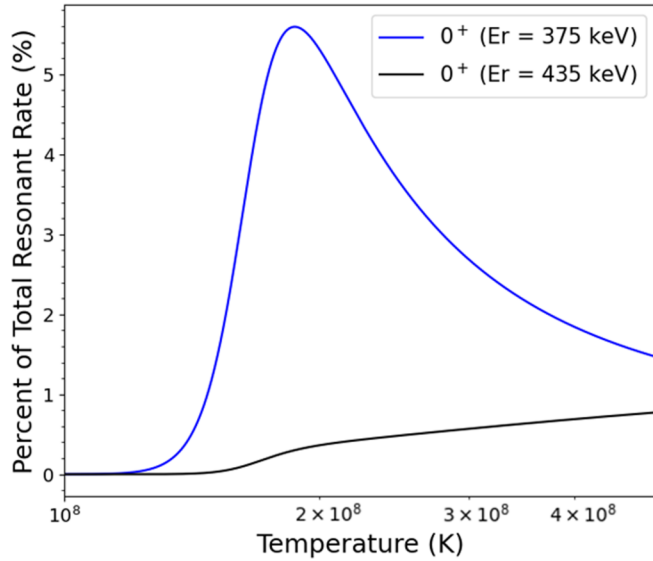


FIG. 8. Contribution of the  $0_4^+$  states to the total  $^{25}\text{Al}(p, \gamma)^{26}\text{Si}$  resonant reaction rate. The relocation of the  $0_4^+$  state, from  $E_{ex} = 5.946$  MeV (in black, Ref. [26]) to  $E_{ex} = 5.889$  MeV (in blue, this work), raises the contribution of the  $0_4^+$  resonance up to  $6 \pm 2\%$ .

calculation of the rate. Therefore, for the calculation of the  $^{25}\text{Al}(p, \gamma)^{26}\text{Si}$  reaction rate, only the  $1_1^+$ , the  $0_4^+$ , and the  $3_3^+$  resonances are taken into account.

The proton-partial widths for the  $1_1^+$  and  $0_4^+$  states are obtained from the work by Wrede [17] and Hamill *et al.* [31], respectively. The  $\gamma$ -partial widths of the  $1_1^+$  and  $0_4^+$  states were obtained from the work of Richter *et al.* [30], after updating the  $\Gamma_\gamma$  value for the  $0_4^+$  which depends on the energy of the transition [17]. The difference is due to the location of the  $0_4^+$  from  $E_{ex} = 5.946$  MeV [30] to  $E_{ex} = 5.889$  MeV measured in this work, giving  $\Gamma_\gamma(0_4^+) = 7.49$  meV.

A comparison of the contribution due to the  $0_4^+$  resonance rate is shown in Fig. 8, where the energy level and the corresponding proton- and scaled  $\gamma$ -partial width of the resonance is used from this work (blue), and the parameters used in Ref. [26] (black). It is observed that by moving the location of the state to  $E_{ex} = 5.889$  MeV, the total resonant rate contribution from the  $0_4^+$  is increased up to  $6 \pm 2\%$  of the total resonance rate, which agrees with the contribution percentage reported by Ref. [31]. For the  $3_3^+$  state, the proton-partial width ( $\Gamma_p$ ) by Peplowski *et al.* [13] is used along with the  $\Gamma_\gamma$  value derived in this work.

The resonance parameters used for the calculation of the  $^{25}\text{Al}(p, \gamma)^{26}\text{Si}$  reaction rate are summarized in Table III. The total and individual contributions of each resonance are shown in Fig. 9, along with the contribution from the direct-capture (DC) to bound states obtained from the work of Iliadis *et al.* [28]. The DC contribution to the reaction rate dominates at temperatures lower than 0.053 GK, the  $1_1^+$  state dominates the reaction rate from  $T = 0.053$  GK–0.177 GK, and at higher temperatures (0.2 GK–0.4 GK) the  $3_3^+$  resonance dominates with contributions from the  $0_4^+$  up to 6% of the total resonant reaction rate.

TABLE III. Resonance parameters for the low-lying proton unbound states in  $^{26}\text{Si}$  observed in this work used in the present calculation of the  $^{25}\text{Al}(p, \gamma)^{26}\text{Si}$  reaction rate. The resonance energies ( $E_r$ ) were calculated using a proton threshold of  $S_p = 5514$  keV [16].

| $E_{ex}$ (keV) | $E_r^a$ (keV) | $J^\pi$ | $\Gamma_p$ (meV)                     | $\Gamma_\gamma$ (meV) | $\omega\gamma$ (meV) |
|----------------|---------------|---------|--------------------------------------|-----------------------|----------------------|
| 5676(3)        | 162(3)        | $1_1^+$ | $4.6 \times 10^{-6} \pm_{3.1}^{9.3}$ | 120                   | $1.2 \times 10^{-6}$ |
| 5889(2)        | 375(2)        | $0_4^+$ | $4.2 \pm 1.0$                        | 7.5                   | $2.2 \times 10^{-1}$ |
| 5929(3)        | 415(3)        | $3_3^+$ | $2900 \pm 1000$                      | $71 \pm 32$           | $40 \pm 17$          |

<sup>a</sup>Obtained by using  $S_p = 5514$  keV [16].

The reaction rate obtained in this work was also compared with the most recent recommended rates [17,19,29,34] in the JINA REACLIB database [43]. Figure 10 shows the ratio of the recommended rates to the present rate as a function of the temperature. At peak nova temperatures, good agreement is found between this work and the latest experimental work by Liang *et al.* [19].

## VI. SUMMARY

In summary, we performed a high-sensitivity neutron- $\gamma$ -ray coincidence measurement to study low-lying resonance states in  $^{26}\text{Si}$  via the  $^{24}\text{Mg}(^3\text{He}, n\gamma)^{26}\text{Si}$  reaction. Neutrons from the reaction were measured with the state-of-the-art CATRINA neutron detector array, while  $\gamma$  rays from the de-excitation of states in  $^{26}\text{Si}$  were measured with the HPGe FSU Clover array. States in  $^{26}\text{Si}$  above the proton-decay threshold ( $S_p = 5.514$  MeV) are critical to the calculation of the  $^{25}\text{Al}(p, \gamma)^{26}\text{Si}$  reaction rate. The high sensitivity of the present experiment allowed us to solve long lasting discrepancies in the existence and location of the important resonances in  $^{26}\text{Si}$ , relevant at nova temperatures.

For instance, the existence and location of the  $0_4^+$  was placed at  $E_{ex} = 5889(2)$  keV in disagreement with the work

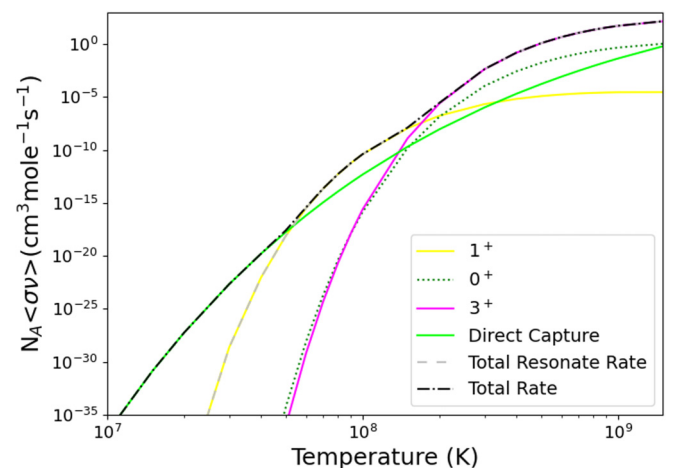


FIG. 9. Rate of the  $^{25}\text{Al}(p, \gamma)^{26}\text{Si}$  reaction calculated in this work. The total and individual contributions of the three resonances within the Gamow window for nova temperatures are shown along with the direct-capture contribution obtained from Ref. [28].

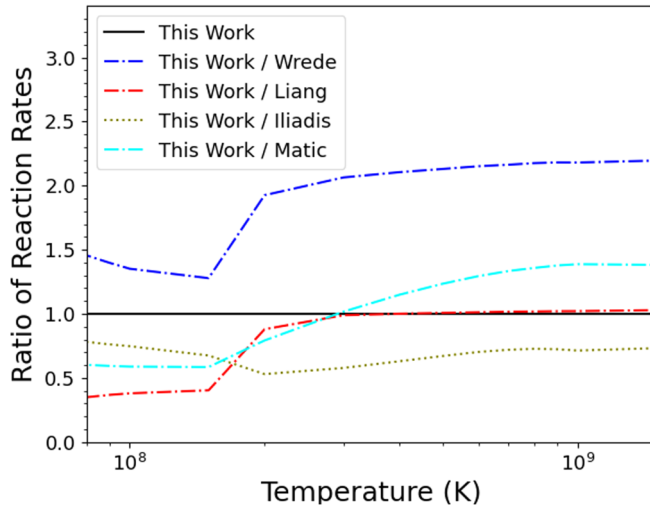


FIG. 10. Comparison of the present calculated reaction rate (numerator) to those reported by Wrede [17], Liang *et al.* [19], Iliadis *et al.* [29], and Matic *et al.* [34] (blue, red, green, and cyan, respectively) in the JINA REACLIB database [43] (denominator).

by Parpottas *et al.* [26], but in agreement with other ( $^3\text{He}, n$ ) experiments [22,24,25]. The contribution of the  $0_4^+$  to the total calculated reaction rate is up to  $6 \pm 2\%$  higher than the one calculated in Ref. [26].

The critical resonance parameters of the  $3_3^+$  resonance, which dominate the reaction rate at nova peak temperatures, extracted from this work were found to be in agreement with recent  $\beta$ -decay studies [17,19], and in rough agreement with a lifetime study of the mirror state in  $^{26}\text{Mg}$  [27]. In the present experiment, we did not find evidence for  $\gamma$  transitions corresponding to a state at  $E_{ex} \approx 5.95$  MeV in  $^{26}\text{Si}$ . This result

is in disagreement with the location of the  $0_4^+$  suggested by Ref. [26] and with the existence of the  $1_1^-$  state suggested by Ref. [27]. Further experiments are needed to confirm the existence or not of a state at  $E_{ex} \approx 5.95$  MeV in  $^{26}\text{Si}$ . It is possible that if a state at 5.95 MeV did exist and it has a very small  $\gamma$  width, then the present experiment would not have the sensitivity to observe it. A possible high-sensitivity study, such as a  $^{24}\text{Mg}(^3\text{He}, np)$ , could provide additional data on the existence of this state.

The largest uncertainty in the calculation of the rate in this work arises from the relative cross-section between the  $0^+$  and the  $3^+$  obtained from the work of Ref. [26]. Further experimental data on the  $^{24}\text{Mg}(^3\text{He}, n)$  reaction at the same beam energy, which focus on the total width of the resonance states, will be needed to confirm these results.

The total reaction rate calculated in this work using the updated values is in good agreement with the previous recommended experimental rates [19] in the JINA REACLIB database [43] at relevant nova temperatures.

#### ACKNOWLEDGMENTS

This work was supported by the Stewardship Science Academic Alliance through the CENTAUR Center of Excellence under Grants No. DE-NA0003841, the National Science Foundation under Grants No. PHY-1712953 and No. PHY-2012522, U.S. Department of Energy Grant No. DE-FG02-96ER40978, and Florida State University. A target provided by the Center for Accelerator Target Science at Argonne National Laboratory was used in this work. We acknowledge the support of D. Caussyn, P. A. Barber and B. Schmidt, R. Boisseau, and J. Aragon at the John D. Fox accelerator laboratory and instrument shop at Florida State University.

- 
- [1] N. Prantzos and R. Diehl, *Phys. Rep.* **267**, 1 (1996).  
 [2] T. Lee, D. A. Papanastassiou, and G. J. Wasserburg, *Astrophys. J. Lett.* **211**, L107 (1977).  
 [3] J. Jose *et al.*, *Astrophys. J.* **612**, 414 (2004).  
 [4] R. Diehl *et al.*, *Astron. Astrophys.* **298**, 445 (1995).  
 [5] L. Bouchet, *PoS ICRC2015*, 896 (2016).  
 [6] N. T. Kita *et al.*, *Chondrites and the Protoplanetary Disk*, Vol. 341 of Astronomical Society of the Pacific Conference Series (Astronomical Society of the Pacific, 2005), p. 558.  
 [7] R. Diehl *et al.*, *Nature (London)* **439**, 45 (2006).  
 [8] R. Diehl, *AIP Conf. Proc.* **1852**, 040004 (2017).  
 [9] I. Nofar, G. Shaviv, and S. Starrfield, *Astrophys. J.* **369**, 440 (1991).  
 [10] K. De *et al.*, *Astrophys. J.* **912**, 19 (2021).  
 [11] J. Jose and M. Hernanz, *Astrophys. J.* **494**, 680 (1998).  
 [12] J. Jose, A. Coc, and M. Hernanz, *Astrophys. J.* **520**, 347 (1999).  
 [13] P. N. Peplowski, L. T. Baby, I. Wiedenhover, S. E. Dekat, E. Diffenderfer, D. L. Gay, O. Grubor-Urošević, P. Hoffich, R. A. Kaye, N. Keeley, A. Rojas, and A. Volya, *Phys. Rev. C* **79**, 032801(R) (2009).  
 [14] C. Iliadis *et al.*, *Astrophys. J. Suppl. Series* **193**, 16 (2011).  
 [15] F. Hammache and N. de Sérville, *Frontiers in Physics* **8**, 630 (2021).  
 [16] M. Wang, W. J. Huang, F. G. Kondev, G. Audi, and S. Naimi, *Chin. Phys. C* **45**, 030003 (2021).  
 [17] C. Wrede, *Phys. Rev. C* **79**, 035803 (2009).  
 [18] K. A. Chipps, *Phys. Rev. C* **93**, 035801 (2016).  
 [19] P. F. Liang *et al.*, *Phys. Rev. C* **101**, 024305 (2020).  
 [20] D. Seweryniak, P. J. Woods, M. P. Carpenter, T. Davinson, R. V. F. Janssens, D. G. Jenkins, T. Lauritsen, C. J. Lister, J. Shergur, S. Sinha, and A. Woehr, *Phys. Rev. C* **75**, 062801(R) (2007).  
 [21] K. A. Chipps, D. W. Bardayan, K. Y. Chae, J. A. Cizewski, R. L. Kozub, J. F. Liang, C. Matei, B. H. Moazen, C. D. Nesaraja, P. D. O'Malley, S. D. Pain, W. A. Peters, S. T. Pittman, K. T. Schmitt, and M. S. Smith, *Phys. Rev. C* **82**, 045803 (2010).  
 [22] N. De Sérville *et al.*, *PoS NIC XI*, 212 (2011).  
 [23] M. B. Bennett, C. Wrede, K. A. Chipps, J. Jose, S. N. Liddick, M. Santia, A. Bowe, A. A. Chen, N. Cooper, D. Irvine, E. McNeice, F. Montes, F. Naqvi, R. Ortez, S. D. Pain, J. Pereira, C. Prokop, J. Quaglia, S. J. Quinn, S. B. Schwartz *et al.*, *Phys. Rev. Lett.* **111**, 232503 (2013).  
 [24] T. Komatsubara *et al.*, *Eur. Phys. J. A* **50**, 136 (2014).



- [25] D. T. Doherty, P. J. Woods, D. Seweryniak, M. Albers, A. D. Ayangeakaa, M. P. Carpenter, C. J. Chiara, H. M. David, J. L. Harker, R. V. F. Janssens, A. Kankainen, C. Lederer, and S. Zhu, *Phys. Rev. C* **92**, 035808 (2015).
- [26] Y. Parpottas, S. M. Grimes, S. Al-Quraishi, C. R. Brune, T. N. Massey, J. E. Oldendick, A. Salas, and R. T. Wheeler, *Phys. Rev. C* **70**, 065805 (2004).
- [27] L. Canete, G. Lotay, G. Christian, D. T. Doherty, W. N. Catford, S. Hallam, D. Seweryniak, H. M. Albers, S. Almaraz-Calderon, E. A. Bennett, M. P. Carpenter, C. J. Chiara, J. P. Greene, C. R. Hoffman, R. V. F. Janssens, J. Jose, A. Kankainen, T. Lauritsen, A. Matta, M. Moukaddam *et al.*, *Phys. Rev. C* **104**, L022802 (2021).
- [28] C. Iliadis, L. Buchmann, P. M. Endt, H. Herndl, and M. Wiescher, *Phys. Rev. C* **53**, 475 (1996).
- [29] C. Iliadis, R. Longland, A. E. Champagne, A. Coc, and R. Fitzgerald, *Nucl. Phys. A* **841**, 31 (2010).
- [30] W. A. Richter, B. A. Brown, A. Signoracci, and M. Wiescher, *Phys. Rev. C* **83**, 065803 (2011).
- [31] C. B. Hamill *et al.*, *Eur. Phys. J. A* **56**, 36 (2020).
- [32] D. W. Bardayan, J. A. Howard, J. C. Blackmon, C. R. Brune, K. Y. Chae, W. R. Hix, M. S. Johnson, K. L. Jones, R. L. Kozub, J. F. Liang, E. J. Lingerfelt, R. J. Livesay, S. D. Pain, J. P. Scott, M. S. Smith, J. S. Thomas, and D. W. Visser, *Phys. Rev. C* **74**, 045804 (2006).
- [33] J. Parker, Nuclear structure studies of  $^{44}\text{S}$  and  $^{26}\text{Si}$ , Ph.D. thesis, Florida State University, 2017, p. 111.
- [34] A. Matic, A. M. vandenBerg, M. N. Harakeh, H. J. Wortche, G. P. A. Berg, M. Couder, J. Gorres, P. LeBlanc, S. O'Brien, M. Wiescher, K. Fujita, K. Hatanaka, Y. Sakemi, Y. Shimizu, Y. Tameshige, A. Tamii, M. Yosoi, T. Adachi, Y. Fujita, Y. Shimbara, H. Fujita *et al.*, *Phys. Rev. C* **82**, 025807 (2010).
- [35] J. A. Caggiano, W. Bradfield-Smith, R. Lewis, P. D. Parker, D. W. Visser, J. P. Greene, K. E. Rehm, D. W. Bardayan, and A. E. Champagne, *Phys. Rev. C* **65**, 055801 (2002).
- [36] Eljen Technology, Deuterated ej315, <https://eljentechnology.com/products/liquid-scintillators/ej-315>, accessed March 13, 2022.
- [37] J. F. Perello *et al.*, *Nucl. Instrum. Methods Phys. Res. A* **930**, 196 (2019).
- [38] CAEN, V1725/v1725s, <https://www.caen.it/products/v1725/>, accessed March 13, 2022.
- [39] CAEN, V1730/v1730s, <https://www.caen.it/products/v1730/>, accessed March 13, 2022.
- [40] S. Y. F. Chu, L. P. Ekstrom, and R. B. Firestone, WWW Table of Radioactive Isotopes, The Lund/LBNL Nuclear Data Search, 1999, <http://nucleardata.nuclear.lu.se/toi/>.
- [41] J. F. Perello, Study of low-lying proton resonances in  $^{26}\text{Si}$  and neutron spectroscopic studies with CATRiNA, Ph.D. thesis, Florida State University, 2021, p. 120.
- [42] M. S. Basunia and A. M. Hurst, *Nucl. Data Sheets* **134**, 1 (2016).
- [43] R. H. Cyburt *et al.*, *Astrophys. J. Suppl. Series* **189**, 240 (2010).